16th International Benchmark Workshop on Numerical Analysis of Dams

Theme B: AAR affected dam

Evaluation and prediction of the behaviour of the Beauharnois dam

Formulation by :
Simon-Nicolas Roth
Benjamin Miquel

September 3, 2021

Benchmark Workshop 2022

Formulated by
Simon-Nicolas Roth, ing. Ph.D.
Chef p.i. Expertise barrages et ouvrages régulateurs

Benjamin Miquel, ing. Ph.D.
Ingénieur - Expertise en barrages et ouvrages régulateurs

Hydro-Québec
Direction Expertise Barrages et Infrastructures
Vice-présidence Planification, stratégies, et expertises
75, boul. René-Lévesque ouest 3e étage Montréal, Québec, Canada, H2Z 1A4

Revision history

#	Revision date	Page	Revision description
1	2021-09-03	-	Initial release

Contents

List of Figures

List of Tables

Introduction 1

1.1 Background

The alkali-aggregate reaction (AAR) can cause serious concerns about the integrity of concrete structures. Moreover, the operation of hydraulic structures such as dams, power plants and spillways affected by this reaction can be compromised. To assess the integrity usability of these structures and to predict the long-term performance and the scale of the investments required to keep the structures in safe conditions, it may be necessary to use numerical models.

Due to the complexity of AAR, its multi-physical/multiscale nature and the constantly evolving research on this subject, there is currently no consensus on how to model AAR. The different modelling approaches were classified [1] on the basis of their input parameters as: (1) models based on concrete expansion, (2) models based on internal pressure, (3) models based on the gel production and (4) models based on the ions diffusion-reaction mechanisms. Some of these approaches are limited to small-scale models whereas others can be extended to structural analyses. These later models are generally not accessible to the general public in commercial software. Therefore implementation of the complex physical equations required to properly model the AAR process (damage, reinforcements, moisture transport, thermal effects, chemical reaction, uplift pressures, etc.) is required by the engineering team.

From the dam owner point of view, it is not easy to take a decision involving a major investment on a structure whose sustainability may not be guaranteed by relying on numerical models whose verification and validation (V&V) process [2] may not be carried out rigorously.

In a numerical model, the fundamental physics is coded using proper discretization (e. g. finite volume, finite difference, finite element, etc.) to predict the behaviour of a physical model. These models are used to reduce the time, cost, and risk associated with full-scale testing of products. In model V&V, verification and validation can be defined as [2]:

- Verification is the process of assessing software correctness and numerical accuracy of the solution to a given mathematical model;
- Validation is the process of assessing the physical accuracy of a mathematical model based on comparisons between computational results and experimental data.

The validation process quantifies the credibility and predictive accuracy of a numerical model providing the decision maker with the information necessary for making high-consequence decisions. The fundamental elements that build credibility in computational results can be defined as [2]:

- quality of the analysts conducting the work;
- quality of the physics modelling;
- verification and validation activities;
- uncertainty quantification and sensitivity analyses.

Engineers seeking to develop credible predictive models critically need model V&V guidelines and procedures. Organizations such as Society for Computer Simulation [3], US Department of Defense [4], American Institute of Aeronautics and Astronautics [5], American Society of Mechanical Engineers [6], Los Alamos National Lab [7] have published guidelines on model V&V.

To date, there were many difficulties to have a formal and systematic framework to validate numerical models able to model AAR-affected concrete structures. The assessment of numerical codes has been partially performed within the ICOLD International Benchmark Workshops on Numerical Analysis of Dams, where three benchmark cases were defined:

- 2011 - Valencia, Spain [8]
  - Case: Kariba dam (arch dam)
  - Exercise: Determining adequate swelling law and parameters which allow the best identification with both horizontal and vertical movements of the dam vs time.
  - Number of participants: 9
- 2005 - Wuhan, China [9]
  - Case: Poglia dam (hollow gravity dam)
  - Exercise: Structural behaviour of a large hollow gravity dam, with special reference to the ultimate strength against the hydrostatic load
  - Number of participants: 2
- 2001 - Salzburg, Austria [10]
  - Case: Pian Telessio dam (arch dam)
  - Exercise: Forecast on stress-strain state generated by AAR
  - Number of participants: -

The European project Integrity Assessment of Large Concrete Dams (NW-IALAD) also conducted a series of cases to help AAR numerical model V&V process. More recently RILEM Technical Committee 259-ISR [11] released two sets of problems (first set at the material scale concrete specimens and the second, at the structural scale) with the objective of creating the first step towards the development of a formal approach recognized by the profession to achieve the V&V process to assess AAR numerical models.

This benchmark is proposed to enrich the database of validation cases at the structural scale. Due to the complexity of modelling such complex phenomena at a structural scale, it is our belief that dams affected by AAR for which rigorous monitoring and surveillance activities have been undertaken for many years should be used as validation benchmark to minimally confirm that a given model is able to estimate the observed behavior and damage.

1.2 Objectives of the benchmark

The objective of this benchmark is to perform modelling of a concrete power plant affected by AAR. The data necessary for the calibration of the model are provided and a prediction phase is proposed. Divided into four tasks, a step-by-step method is proposed to integrate the physics affecting the chemical reaction. Participants are invited to provide the displacements at certain topographic points, the resultant forces on given interfaces and to provide certain plots to qualitatively describe the cracking computed.

The phases of the studies are as follows:

- Calibration and prediction (50%): The formulators of the benchmark provide information necessary to perform the time-history studies of the structure, including geometry, details and arrangement of the reinforcement, finite element model, material characteristics, boundary conditions (displacements, thermal and hygral), static loading (self-weight and hydrostatic pressure due to reservoir loads). The participants are expected to analyze the data provided and the required results. They may introduce additional data, and refine the finite element mesh provided if required for the purposes of the envisaged analysis. It is underlined that the current benchmark problem concerns only the concrete body and excludes those related to the dam foundation.
- Results, evaluations and conclusions (30%): The expected results include the temporal displacements, the interface loads history and the structure stiffness change according to the progression of the alkali-aggregate reaction. A number of plots should be provided by the participants to identify the principal cracks. Cross sections are suggested to facilitate understanding and allow comparison with those of the other participants. It is also suggested that the participants comment and explain these results. It is recommended to define the possible failure mechanisms associated with the cracking computed. High emphasis should be given to the engineering interpretation and analysis of the obtained results in view of the dam's safety.
- A critical review of the numerical model (10%): A critical review of the numerical model employed within the context of the benchmark is requested. The participant may discuss the level of physics required to correctly predict the effect of the AAR.
- Proposals for stability and functionality analysis (10%): Participants are asked to give ideas on methods that could be used to evaluate the stability and functionality of the power plant based on computed damage, displacements, etc. Proposals and recommendations for further consideration are requested.

1.3 Brief dam description

The Beauharnois dam is located about 50 km west of the city of Montreal. The power station, with a total length of 1397 m, turbines the waters of the St. Lawrence River and includes 37 turbine-generator units, 36 of which are in service and two auxiliary units A and B out of service for a total installed power of 1903 MW.

The Beauharnois development includes a spillway, left and right bank gravity dams and approximately 50 km of dikes on the left and right banks of the Beauharnois Canal. This canal was built between 1929-1932 on the south side of the St-Lawrence River measuring 24.5 kilometres in length, with a minimum depth of 8 metres and a width of 182 metres. The canal was built to take advantage of the 24 metres drop between Lake St-Francis and Lake St-Louis. The Beauharnois development is part of the Beauharnois-Les Cèdres hydroelectric complex displayed in figure 1.1.

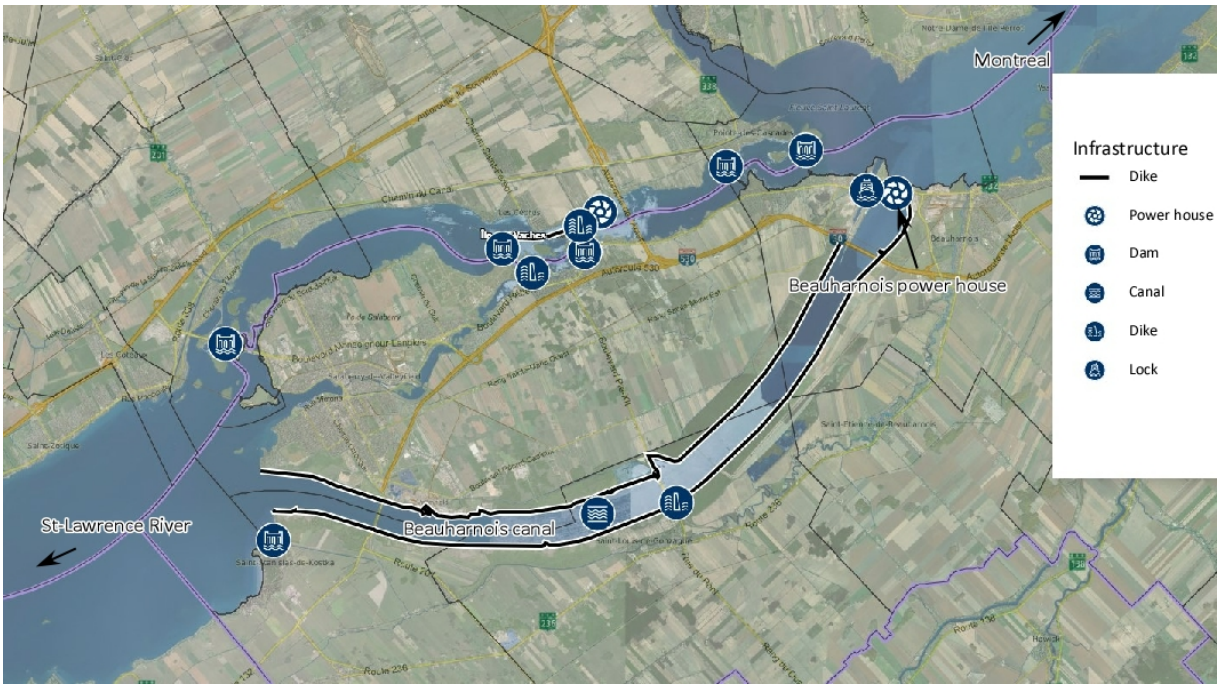

Figure 1.1: Beauharnois-Les Cèdres hydroelectric complex

The construction of the Beauharnois power plant took place in three phases:

- the first phase (phase I) where the concreting of the groups took place in the period 1930-1932 with the commissioning of 14 groups (groups 1 to 14) between 1932 and 1948;
- 12 more groups (from 15 to 26) were put into service between 1950 and 1953 for the second phase (phase II);
- and finally during the third phase of construction (phase III), 10 groups (from 27 to 37) were put into service between 1959 and 1961.

Within the framework of a numerical benchmark, it is not realistic to model the entire power station with a length of 1397 m. Therefore, a single power unit with its two neighbouring units will be considered.

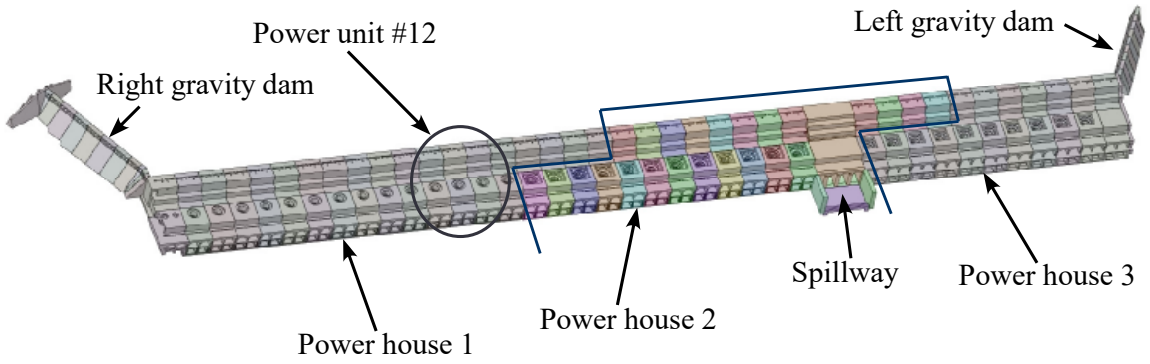

Figure 1.2: Beauharnois power plant

The power unit #12 (illustrated in figure 1.2) was selected because it is reasonable, in the reduced numerical model, to assume symmetric boundary conditions as it is located far from the gravity

dams and spillway sections which influence longitudinal displacements. In addition, this power unit has a more sophisticated auscultation system than other power units. Note that the topographic auscultation system was implemented in 1973, therefore the first 40 years of data was not recorded.

Several decades of investigations and interventions were made to mitigate the effect of AAR. These interventions have low effects on the displacements, therefore they will be ignored for this benchmark.

1.4 Problem statement

The benchmark proposes to calibrate the numerical model of power units #11 to #13 on the basis of the recorded data and to predict the displacements, damage, loads of the next 50 years with different levels of physics affecting the chemical reaction.

The formulators of the benchmark provide information necessary to perform the time-history studies of the structure, including geometry, details and arrangement of the reinforcement, finite element model, material characteristics, boundary conditions (displacements, thermal and hygral), static loading (self-weight and hydrostatic pressure due to reservoir loads).

Divided into four tasks (one mandatory and three optional), the participants are invited to provide the displacements at certain topographic points, the resultant forces on given interfaces and to provide certain plots to qualitatively describe the cracking computed.

1.5 Deliverables

The results provided by the participants will be both in paper format, but also the requested raw output data should be submitted to formulators by an Excel template file.

The paper should present the chosen solution method. The AAR model shall be described along with the method used to couple the physics with the chemical model. The process for performing the V&V of the AAR model should be presented in the document.

It is recommended to define and provide explanation for any additional parameters added to calibrate the model.

The items discussed in the phases of the studies (section 1.2) should be included in the paper. This includes the results, evaluations and conclusions. A section on a critical review of the numerical model is highly recommended. Finally, proposals for stability and functionality analysis shall be discussed.

Numerical model 2

2.1 Coordinate system

The coordinate system to be used by all participant is as follow:

- X direction: bank direction; positive towards right bank;
- Y direction: upstream/downstream direction; positive towards downstream;
- Z direction: vertical direction; positive towards elevation.

All information provided by this benchmark are in this coordinate system.

2.2 Geometry

The power unit #12 is part of the first phase of construction of the Beauharnois power station commissioned in 1932. Figure 2.1 shows a typical cross section of the first phase of construction. The water intake part has a height of approximately 21.5 m and includes the penstocks, the upstream gates and the busbar. The power plant is approximately 24 m high and includes the generator unit, the scroll case, the draft tube, the tailrace and the downstream gates. A cold joint separates the water intake part from the power plant.

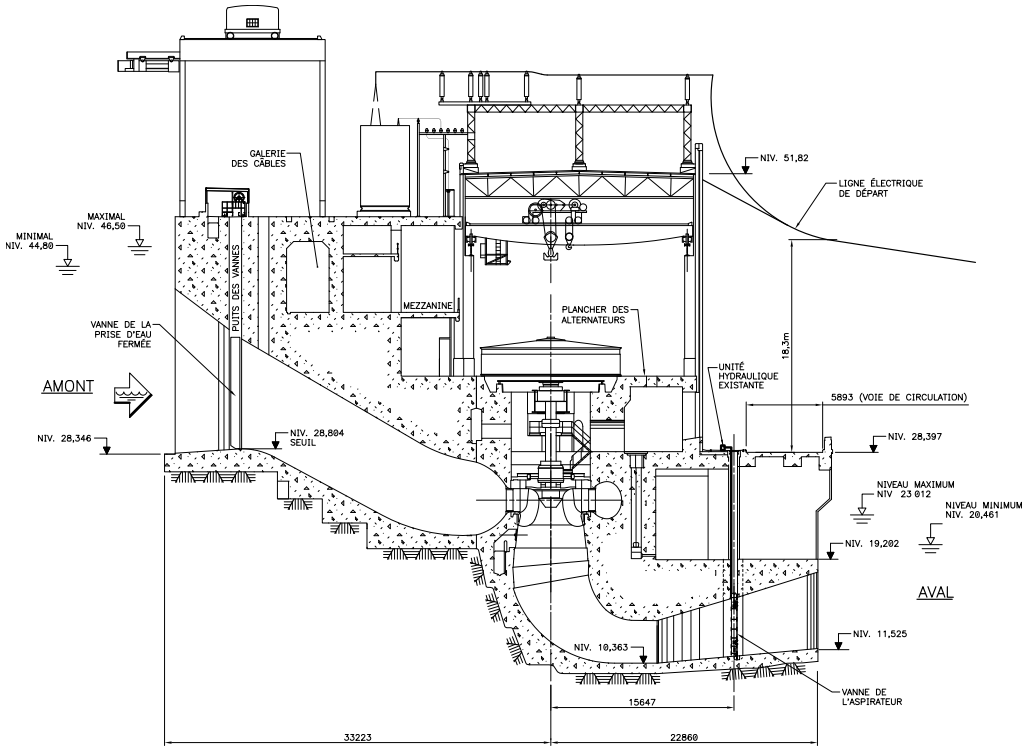

Figure 2.1: Cross section of power unit #12

2.3 Mechanical boundary conditions

The displacement boundary conditions applied to the model (displayed in figure 2.2) are as follows:

- on the base of the foundation, a zero displacement in the 3 directions X, Y, Z is applied (Ux = Uy = Uz = 0);
- on the downstream part of the foundation, a zero displacement in Y is applied (Uy = 0);
- on the right bank and left bank boundaries of the foundation and the dam, the displacement in direction X is blocked (Ux = 0).

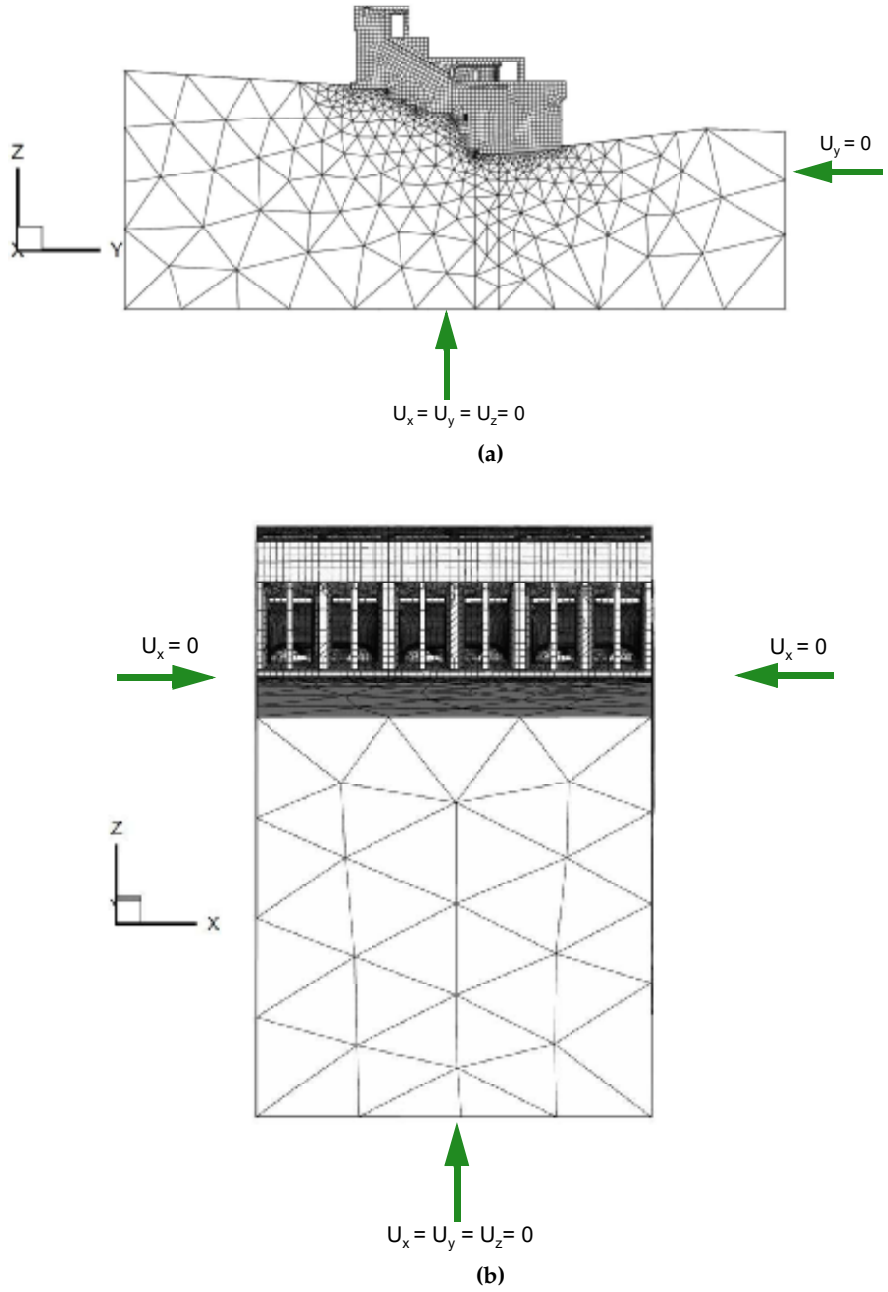

Figure 2.2: (a) Downstream and foundation boundary conditions, (b) Lateral and foundation boundary conditions

2.4 Thermal boundary conditions

Heat transfer analyzes are needed if the AAR kinetic model explicitly requires the temperature field. These allow to compute the temperature field within the dam. The temperature field can then be used as an input for mechanical analysis where the temperature of the concrete can greatly influence the kinetics of AAR.

It is recommended to use the same numerical model for heat transfer and for mechanical analysis. Heat transfer analyzes can be carried out in a transient regime over a sufficiently long period (by experience, about 6 years are required considering an initial nodal temperature value corresponding to the average outside temperature) to allow convergence (repetition of temperature variations year after year). The computed sixth year can be used repeatedly for mechanical analysis. However, any other method can be used.

The boundary conditions are defined in figure 2.3 and the corresponding annual temperature distribution (colour code) is displayed in figure 2.4. The excel file provided in the *Temperature.xls* package gives the numerical values displayed in the figure. The convective coefficient associated with each annual temperature distribution is given in table 2.1.

No temperature must be applied at the concrete-rock interface, on the left and right banks, on the upstream, downstream and lower foundation limits ensuring free heat exchange. On the upper surface of the foundation located upstream and downstream of the power plant, the water temperature should be applied.

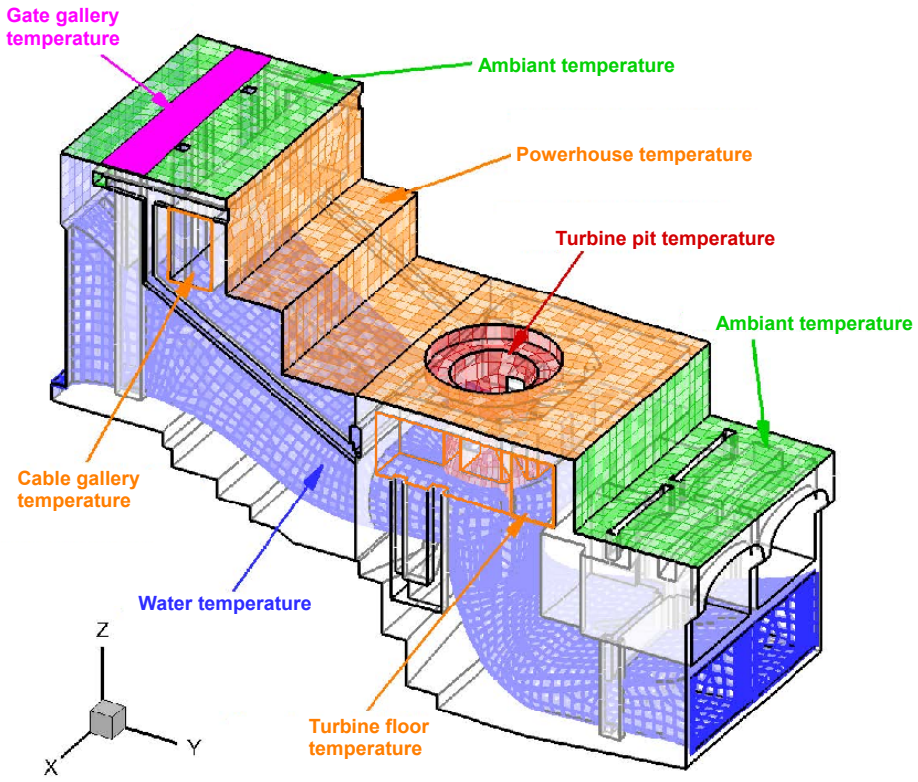

Figure 2.3: Thermal boundary conditions

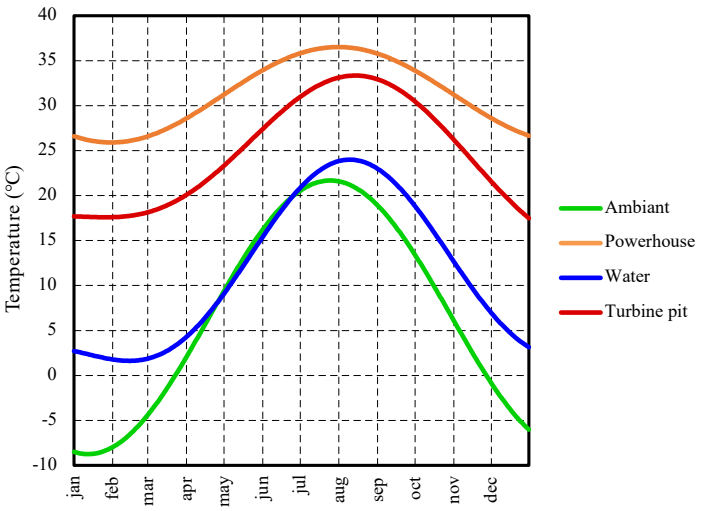

Figure 2.4: Yearly temperature variation

Table 2.1: Temperature boundary conditions

Boundary name	Convection coefficient (W m^{-2} °C^{-1})
Ambient	24.7
Powerhouse/turbine floor	9.5
Water	696.0
Turbine pit	108.0

2.5 Hygral boundary conditions

In a concrete structure, the degree of initial saturation is close to 100% and is reduced by drying and desiccation. The drying modelling is generally based on a nonlinear diffusion equation governing the evolution of liquid water saturation. This equation is similar to a generalized Darcian flow in a transient state. The work of [12], [13], [14] and [15] allow us to solve this equation formulated as a function of capillary pressure.

The boundary conditions are given in figure 2.5 in terms of capillary pressure P_c and relative humidity h_r. These values are based on measured temperatures and humidity levels. The capillary pressure corresponds to the pressure difference between a saturated medium and an unsaturated medium. If the concrete is saturated with water, then there is no capillarity phenomenon and therefore this pressure is zero. Conversely, if the air is very dry, the pressure required to penetrate the low humidity must be very high. This pressure is given by equation 2.1.

$$P_c = \left(-\frac{\rho RT}{M_l}\right) \ln h_r \tag{2.1}$$

where T is the ambient air temperature in Kelvin (°C + 273), h_r the relative humidity, r and M_l are the volumetric (1.106 g/m^3) and molar (18.015 g/mol) masses of water , and R is the ideal gas constant, 8.314 J/mol/K.

The capillary pressures given are based on the average temperature recorded near the boundary.

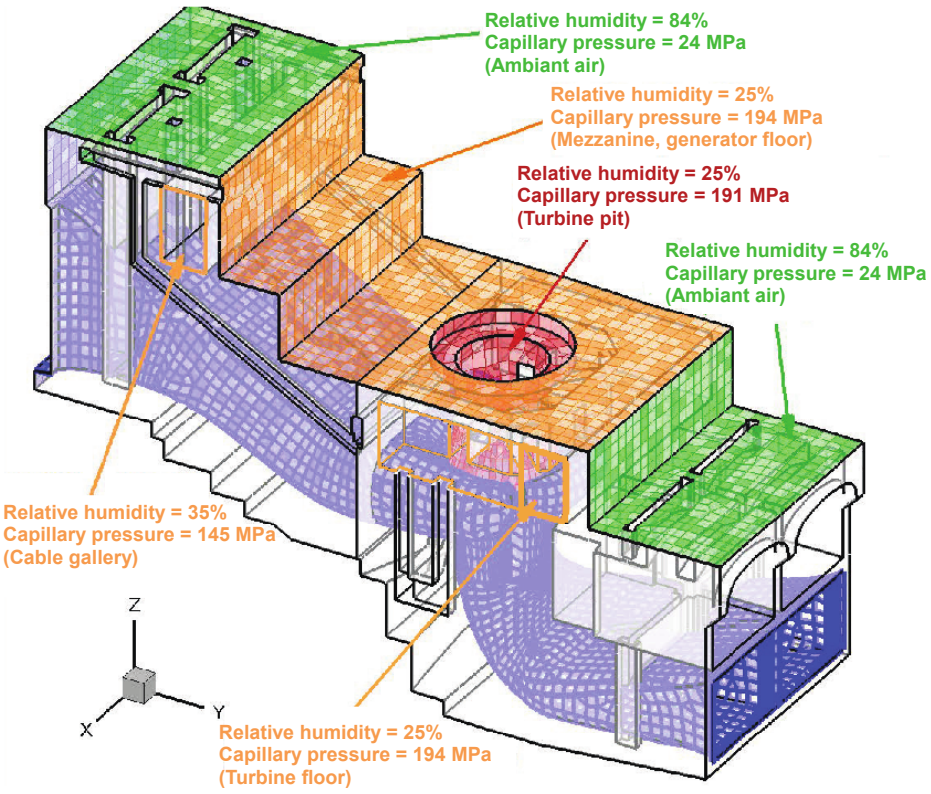

Figure 2.5: Hygral boundary conditions

2.6 Concrete reinforcement

Three different types of steel were used for the structural steel for the Beauharnois generating station:

- type HG for "Hard Grade";
- type SG for "Structural Grade";
- type IG for "Intermediate Grade".

Table 2.2 presents the steel properties for each grade.

Table 2.2: Reinforcement steel properties

Property	Tensile strength (F_y) (MPa)	Ultimate strength (F_u) (MPa)
Hard Grade	345	552
Structural Grade	228	397
Intermediate Grade	276	483

For groups 11, 12 and 13, rebars of 0.75 inch (19 mm), 1 inch (25.4 mm), 1.25 inch (31.75 mm) and 1.5 inch (38 mm) were used with square or round sections (given in figure 2.6). The steel elastic modulus is 200 GPa. The participants are free to model the reinforcements using embedded, smeared or discrete formulations.

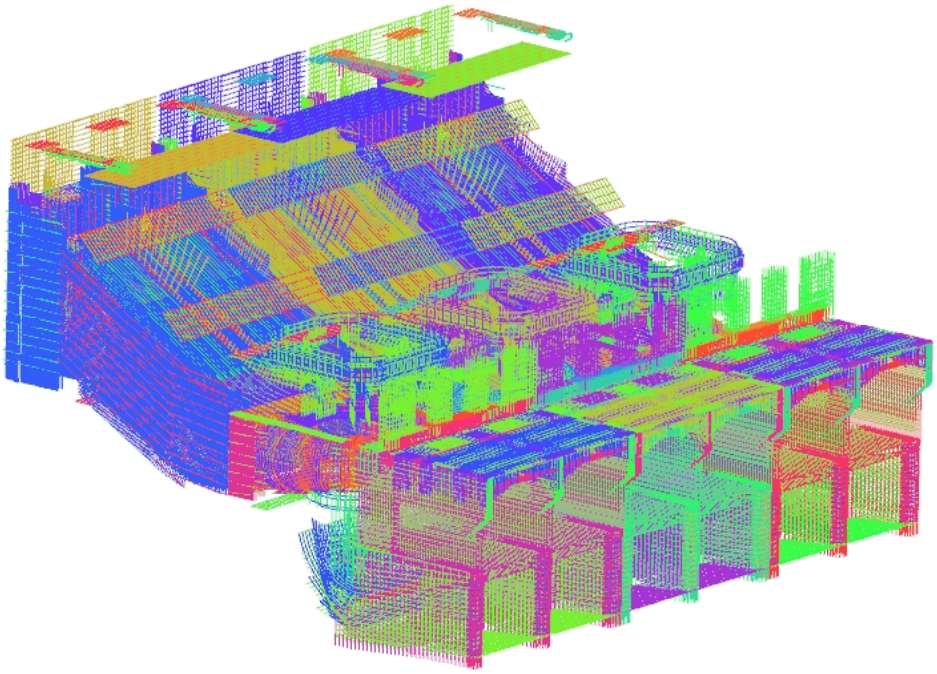

Figure 2.6: Concrete reinforcement

2.7 Material properties

The material properties used for the mechanical analyzes were determined in part using: empirical formulas from the literature, the characteristics of the concrete used during the different construction phases of the Beauharnois development and the multiple investigations and tests carried out over the years. Properties which could not be obtained from these sources were evaluated using sensitivity studies. The review of construction documentation, the concrete investigations and laboratory tests show that the same concrete was used in both intake and powerhouse structures. Therefore, participants should use identical chemical reaction properties for unconfined concrete at identical temperature and humidity in these two structures. Table 2.3 presents the material properties to be used for the numerical analysis while table 2.4 gives the resistance parameters used for the material performance during nonlinear analyzes.

Table 2.3: Material properties

Property	**Concrete**	**Foundation**
Density (kg/m^3)	2365	0 (mechanical analysis) 2627 (thermal analysis)
Poisson's ratio (ν)	0.21	0.20
Instant modulus (GPa)	26	-
Deformation Modulus (GPa)	-	30
Specific heat (J/kg °C)	917	800
Coefficient of thermal expansion (°C^{-1})[a]	0	0
Thermal conductivity (W/m °C)	2.9	4.3
Reference temperature (°C)	10	4

[a] To simplify the analysis, the thermo-mechanical effects are not considered.

Table 2.4: Concrete strength properties

Property	**Value**
Compressive strength (f'_c) (MPa)	30
Tensile strength (f_t) (MPa)	3
Fracture energy (G_F) (N/m)	350

The concrete hygral properties are defined in table 2.5 and are related to the Mualem model [14] for desorption. The foundation is considered fully saturated.

Table 2.5: Concrete hygral properties

Property	**Value**
Initial saturation	0.85
Parameter a (MPa)	18.6
Parameter m	0.44
Total porosity ϕ (m^3/m^3)	0.14
Absolute or intrinsic permeability k (m^2)	5.49×10^{-12}

Requested analyzes 3

3.1 Mechanical analyses

The mechanical analyses are required to compute stresses and displacements in the dam. These time-dependent analyses may be performed as static or quasi-static depending on the preferences of the participant. The loads that should be considered in the analyses are:

- gravity loads;
- hydrostatic water pressure;
- induced load caused by the chemical reaction.

All mechanical analyzes are started on July 1, 1932 and the calibration period ends on January 1, 2017. The data available to calibrate the model does not cover the entire period. Therefore, to calibrate the model, it is suggested to shift the data to match the total displacement computed on the first day of acquisition. Finally, participants are free to define the time step of their choice.

The temperature distributions obtained from the thermal analysis should be used as input to the analysis only to consider its influence on the chemical reaction. It is required to neglect the thermo-mechanical effects by setting the coefficient of thermal expansion $\alpha = 0$ for all materials as previously defined in table 2.3.

Gravity loads

The gravity load for the concrete dam should be included in all analyses based on the densities given in table 2.3. No gravity load or density should be considered for the foundation.

Hydrostatic water pressure

Hydrostatic water pressure should be included in all analyses. The upstream water level should be 46.10 m and the downstream water level should be 21.4 m. The penstocks, scroll case, draft tube and tailrace pressure is considered to vary linearly between the upstream and downstream level.

Induced load caused by the chemical reaction

All types of models, from the simplest to the most complex, can be used by the participants (thermal analogy, poroelasticity, multi-physics, chemo-mechanical, etc.). The considered model must be documented and presented in the paper.

3.2 Other considerations

In addition, all participants also have the possibility to include other specific aspects or assumptions that is believed to improve the analysis. The participants can use unbound interfaces between the power units and between the water intake part and the power unit. The type of physical coupling (one-way or two-way coupling) depends on the preferences of the participant. These can be documented and presented in the paper.

Creep and relaxation

The participants may choose to consider the effect of creep and relaxation in the analyses. Creep and relaxation have a significant influence on the state of stress due to induced AAR strains. A viscoelastic or viscoplastic rheological model can be introduced by the participants to convert swelling strain into realistic stress values. It is expected that the inclusion of creep and relaxation in the analyzes will reduce the damage, diffuse cracking, increase the crack openings and increase the displacements.

In the absence of creep tests which last several months or even years in order to obtain an asymptotic strain curve, it is recommended to use a creep modulus of 0.5 times the initial elastic modulus of concrete. This value comes from tests carried out on an American dam [16] and on cores extracted from another Hydro-Quebec owned dam.

3.3 Linear task (mandatory)

Prior to achieve the nonlinear tasks, the participants shall perform a static linear elastic analysis. Only the dead load and hydrostatic pressure shall be imposed. If the participants want to use unbound interfaces between the different power units and between the water intake part and the power unit, it is required to bound them for this analysis. In addition, no creep or relaxation shall be considered for this analysis.

3.4 Nonlinear tasks

Four tasks are proposed for this theme, with one mandatory (A) and the other three considered as optional (B, C, D). Figure 3.1 gives the proposed path to achieve the tasks. The participant can bypass a task, however it is recommended to integrate the physics in the proposed order. For example, if a model does not consider the effects of the concrete saturation on the chemical reaction, participants can integrate the physics of tasks A and B without considering that of task C when task D is performed. The tasks are described in the next sections.

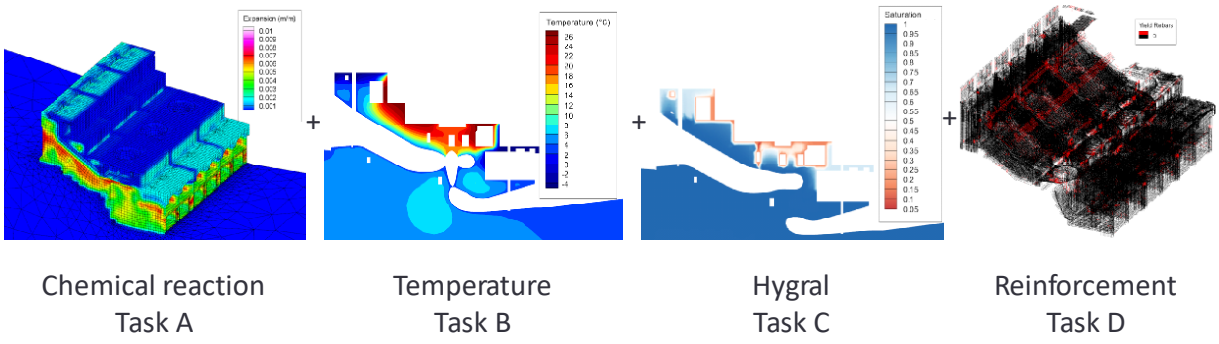

Figure 3.1: Tasks for theme B

3.5 Task A: Baseline solution (mandatory)

The baseline solution is considered to be the simplest of the four nonlinear tasks. The induced load caused by the chemical reaction is computed using a uniform and constant thermal field at 10 °C and the concrete must be considered to be fully saturated.

The calibration shall be carried out with the measured data and a prediction of 50 years up to January 1, 2067 is requested. Since the boundary conditions in the longitudinal direction (X component) is imposed and considered as zero, displacements in this direction shall not be compared to the measured data.

The instrumentation data available to calibrate the model does not start at the end of the construction period. The total displacement is therefore unknown. Thus, as the real displacement at the start of the acquisition period is not zero, the measured data must be translated for calibration. This translation value will be a function of the latency time imposed by the swelling model, on the variation of the concrete stiffness, on the state of damage, etc.

3.6 Task B: Consideration of thermal effects (optional)

The thermal effects are important on the latency time as well as on the rate of swelling. For a structure subject to a northern climate, areas exposed to ambient air should swell at rates lower than those found near power units. By carrying out a thermal study in transient mode (by a coupled or decoupled analysis), it is suggested to take the steps of the baseline analysis again, but by imposing the computed thermal field. Two methods can be used: (1) determine the mean nodal thermal field and impose it during the analysis (2) vary the thermal field as a function of time during the analysis. This analysis should be carried out by repeating the phases of calibration and prediction from rhe previous task.

3.7 Task C: Consideration of hygral effects (optional)

By taking the steps of the previous tasks, a sensitivity analysis of the results according to the distribution of the degree of saturation of the concrete should be carried out. By carrying out a nonlinear transient diffusion (by a coupled or decoupled analysis), it is suggested to take the steps of the previous tasks again, but by imposing the computed hygral field. Similarly to task B, two

methods can be used: (1) determine the steady hygral field and impose it during the analysis (2) vary the hygral field as a function of time during the analysis. This analysis should be carried out by repeating the phases of calibration and prediction and optionally by integrating the physics of the previous tasks.

3.8 Task D: Consideration of reinforcement (optional)

The confinement effects caused by the presence of reinforcement have an influence on the rate of swelling, diffusion of cracks, reduction in cracks openings, etc. Task D therefore consists of taking into account the presence of reinforcement. This analysis should be carried out by repeating the phases of calibration and prediction and optionally by integrating the physics of the previous tasks.

3.9 Summary of the tasks

Table 3.1 gives a summary of the physic integration for each proposed tasks. The requested results are given in the next section.

Table 3.1: Physic integration

		Task	Dead load	Hydrostatic load	Thermal effects	Hygral effects	Reinforcement
Static	Linear	Initial	X	X	-	-	-
Time-History	Non-Linear	A	X	X	-	-	-
		B	X	X	X	-	-
		C	X	X	O	X	-
		D	X	X	O	O	X

X: Mandatory
O: Optional

Requested results 4

4.1 Topographic point location

The location of the topographic point for model calibration and prediction period are illustrated in figure 4.1 and located at these coordinates:

- Crest : monitoring point identified as 1250D160 (901.9829, 1194.1149, 48.9311);
- Turbine pit : monitoring point identified as 1295Q099 (893.4600, 1217.970000, 30.1341);
- Turbine floor : monitoring point identified as 1250U097 (902.3079, 1230.1218, 29.3903).

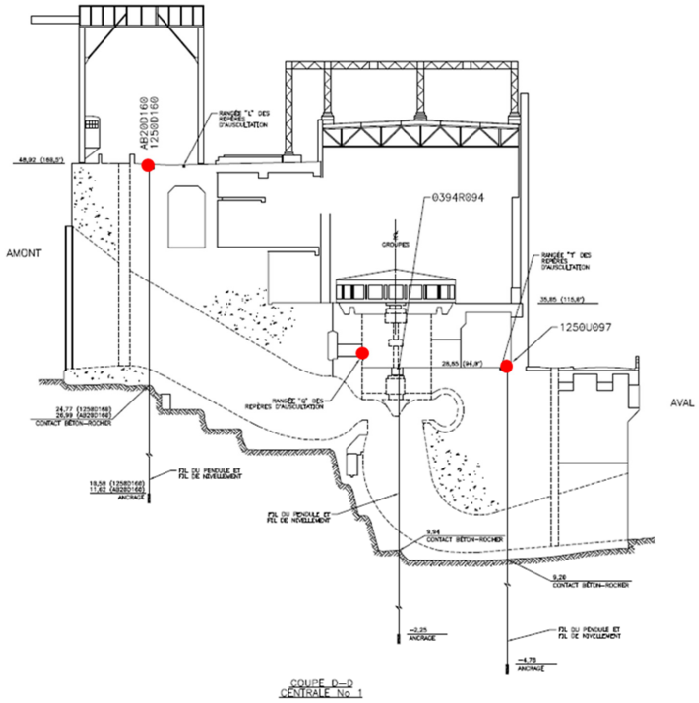

Figure 4.1: Topographic point and pendulum location (highlighted in red)

4.2 Displacements

For the topographic points given in section 4.1, the participants shall record the upstream/downstream (Y component) and vertical (Z component) in a table similar to table in the provided file.

Table 4.1: Results at topographic points

Topographic point	Y (mm)	Z (mm)
1250D160	X	X
1295Q099	NA	X
1250U097	X	X

4.3 Displacements time histories

The participants shall present the upstream/downstream (Y component) and vertical (Z component) time-history displacements for the entire result range (from July 1, 1932 up to January 1, 2067) in the provided file for the topographic points given in section 4.1.

4.4 Resultant forces at the interface

Participants shall output the resultant forces at different interfaces of power unit #12. The interfaces are displayed in figure 4.2 and the results should be recorded in a table similar to the table 4.2 provided in the provided file.

For comparison purposes, the resultant on one interface should ignore nodal forces located at the junction between two interfaces as follow:

- Intake 11/12 & 12/13: all nodal forces on this interface except those located at bedrock and intake/unit interface;
- Unit 11/12 & 12/13: all nodal forces on this interface except those located at bedrock and intake/unit interface;
- Intake/Unit: all nodal forces on this interface except those located at bedrock;
- Rock/Intake & Rock/Unit: all nodal forces on these interfaces.

Table 4.2: Results at the interfaces of power unit #12

Interface	X (MN)	Y (MN)	Z (MN)
Intake 11-12 (purple)	X	X	X
Intake 12-13 (cyan)	X	X	X
Intake/Unit (orange)	X	X	X
Unit 11-12 (brown)	X	X	X
Unit 12-13 (red)	X	X	X
Rock/intake (green)	X	X	X
Rock/unit (pink)	X	X	X
Sum left bank	X	X	X
Sum right bank	X	X	X
Sum rock-concrete	X	X	X

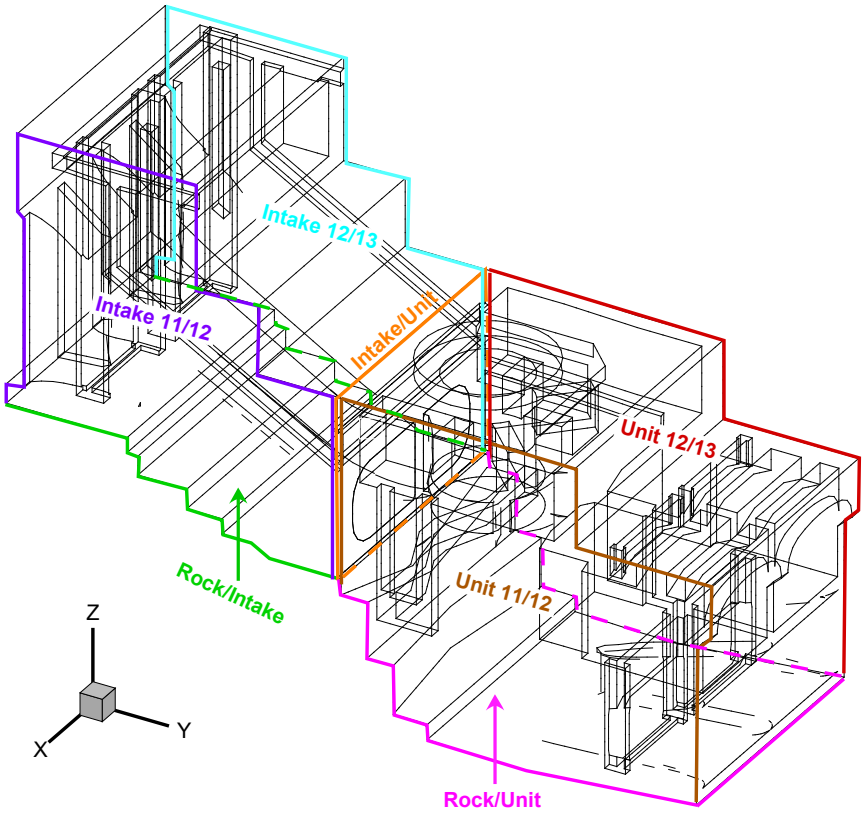

Figure 4.2: Illustration of the forces at the interfaces - power unit #12

4.5 Resultant forces at the interface time histories

Participants shall present the time-history resultant forces at the seven proposed interfaces of power unit #12 for the entire result range (from July 1, 1932 up to January 1, 2067) in the provided file.

4.6 Reservoir drawdown

As the stiffness of the dam changes according to the progression of the alkali-aggregate reaction, it is proposed to compare the upstream/downstream displacements at the crest of the dam (topographic point 1250L160) between two states. Sustained variation (including reversible creep) of a 5-meter water drawdown will allow comparison of the stiffness of the participants models after a swelling analysis over a defined period. For comparison purposes, this same variation in water level should be applied to a model not taking into account the alkali-aggregate reaction in order to compare with the initial stiffness of the dam. In summary, the following four steps are required:

1. Define Y_1: steady analysis with an upstream water level of 46.10 m and a downstream level of 21.4 m;
2. Define Y_2: reduction of the upstream level by 5 m (41.10 m);
3. Define Y_3: transient swelling analysis until January 1, 2017 with a water level of 46.10 m upstream and a downstream level of 21.4 m;
4. Define Y_4: reduction of the upstream level by 5 m (41.10 m).

To recover the effect of a reservoir drawdown level on the dam movements (step 2 and 4), it is recommended to continue the analysis for a period of 10 years by applying an instantaneous reduction in the water level on January 2, 2017. This period extension is carried out with the aim of recovering the displacements considering reversible and irreversible creep effects (if considered).

Figure 4.3 gives an example of the two analyses required to compute the stiffness change. Prior to AAR, the hydrostatic and body loads are applied on July 1, 1932. These loads are left constant until the displacement has reached an asymptotic value (creep). Thereafter the upstream water level is lowered by 5 m and creep recovery occurs until asymptotic value is reached. Both asymptotic values are recorded (values Y_1 and Y_2).

After the time-history analysis is performed between July 1, 1932 and January 1, 2017, the crest displacement is recorded (value Y_3). On January 2, 2017, the water is lowered by 5 m and the crest displacement is recorded after 121 days (value Y_4). The difference Y_3/Y_1 and Y_4/Y_2 gives respectively instantaneous and sustained stiffness variation.

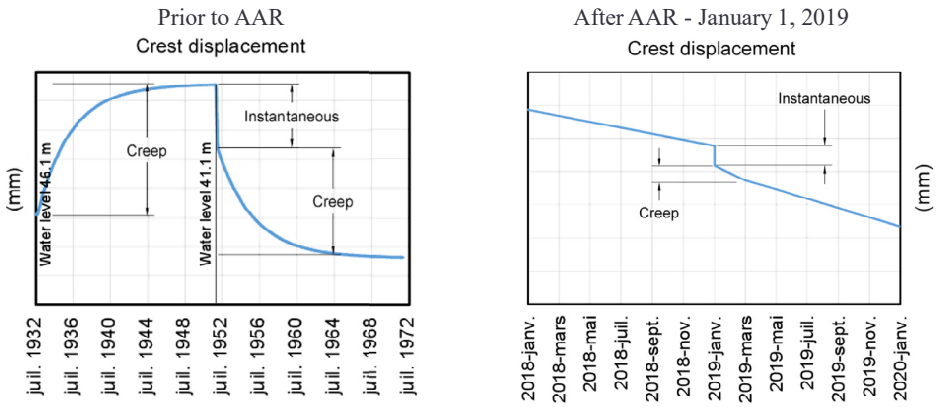

Displacement	Y (mm)
Instantaneous	Y_1
After creep recovery	Y_2

Displacement	Y (mm)
Instantaneous	Y_3
After 2 time steps (121 days)	Y_4

Diff
Y_3 / Y_1
Y_4 / Y_2

Figure 4.3: Effect of AAR on model stiffness (computation example)

4.7 Qualitative results

Another data that can be used in order to qualitatively compare the different models is to compare the computed cracks. Therefore, it is recommended that participants identify the principal cracks, comment and explain them through different plots. It is recommended to perform an interpretation of the cracks as well as the possible failure mechanisms associated with them. Since it is not trivial to analyze damage or plasticity plots by a member unfamiliar with the constitutive model used by the participants, this analysis phase must be carried out with rigour by the analysis team. Without being limited to the variables associated with damage/plasticity, cracks openings can be presented in order to facilitate understanding and allow comparison with those of the other participants. It is also suggested to provide thermal (summer/winter) and hygral (steady state) distribution at a cross section located at the centre of power unit #12. Examples are given in figure 4.4, where cracks openings, reinforcement bars yielding, thermal and hygral distribution are displayed.

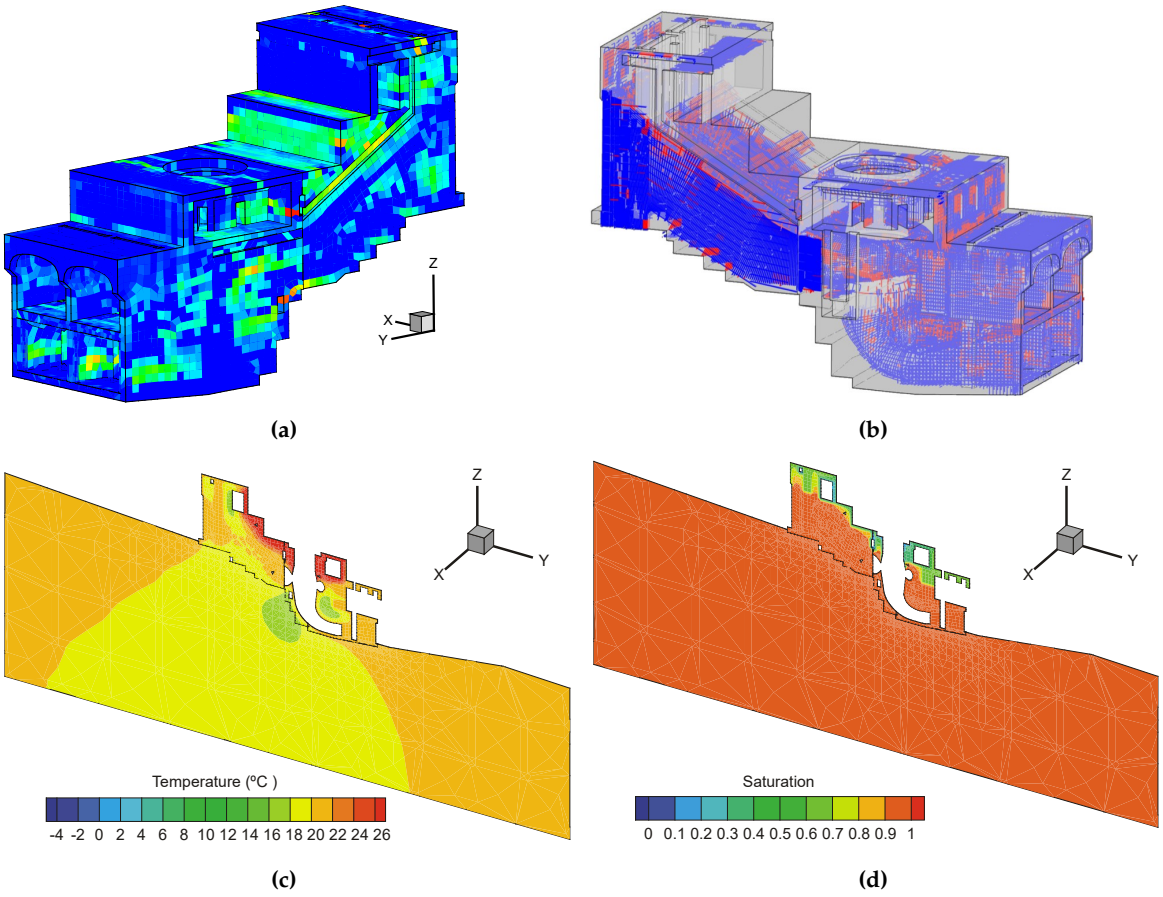

Figure 4.4: (a) Crack opening , (b) Reinforcement bars yielding, (c) Thermal distribution section cut (X=901.36 m), (d) Hygral distribution section cut (X=901.36 m)

4.8 Summary of the requested results for each proposed task

Table 4.3 gives a summary of the requested results for each proposed task.

Table 4.3: Requested results for each task

		Task	Result description section					
			4.2	4.3	4.4	4.5	4.6	4.7
Static	Linear	Initial	X	-	X	-	-	-
Time-History	Non-Linear	A	X[a]	X	X[a]	X	X	O[b]
		B	X[a]	X	X[a]	X	O	O[b]
		C	X[a]	X	X[a]	X	O	O[b]
		D	X[a]	X	X[a]	X	O	O[b]

X: Mandatory
O: Optional

[a] for January 1, 2017
[b] for January 1, 2017 and/or January 1, 2067

List of supplied files 5

5.1 Model geometry

The geometry of the three power units including the foundation is given in STEP and Parasolid file formats. These are provided to participants if, for the purposes of the envisaged analysis, a refinement of the provided finite element mesh is required.

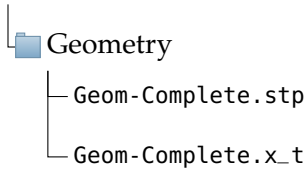

5.2 Finite element mesh

The mesh of the three power units was generated to reproduce the in-situ structure as accurately as possible. The model was not developed to assess the dam foundation. Thus, the foundation is formed by a mesh of coarse tetrahedral elements. Finally, the fineness of the mesh, with elements of approximately 1 m x 1 m x 1 m, was defined so that the computation time for a simulation period of 135 years, using a reasonable time step with an implicit finite element model, can be achieved within the range of one working day. Trilinear form of elements are provided, hence it is recommended to use enhanced strain (or incompatible mode) formulation. The mesh was generated favouring hexahedral elements, however, degenerated elements such as wedge, pyramidal and tetrahedral elements were also generated. The nodal definition of the elements are given in figure 5.1.

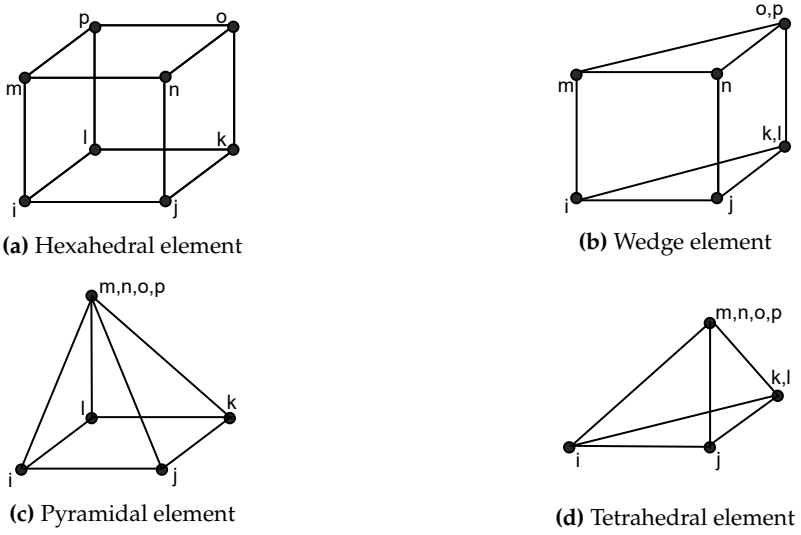

(a) Hexahedral element

(b) Wedge element

(c) Pyramidal element

(d) Tetrahedral element

Figure 5.1: Element shape nodal definition

The finite element mesh includes a total of 271,164 elements and 114,674 nodes. It is required to link certain concrete components together at the interfaces using linear methods (constraint equations, multi-point constraints, bounded contacts, etc) or non-linear methods (contact elements with Mohr-Coulomb formulation, etc.). Taking into account that the nodes at the interfaces do not necessarily coincide, these links shall be applied to the interfaces between the intakes and the generator units and those in the transverse interfaces between the different power units. The interface mesh at the rock/concrete interface is made by making sure that the nodes coincide.

The mesh nodal boundaries, the nodal definitions and the elements topology are distributed in different files according to the following hierarchy:

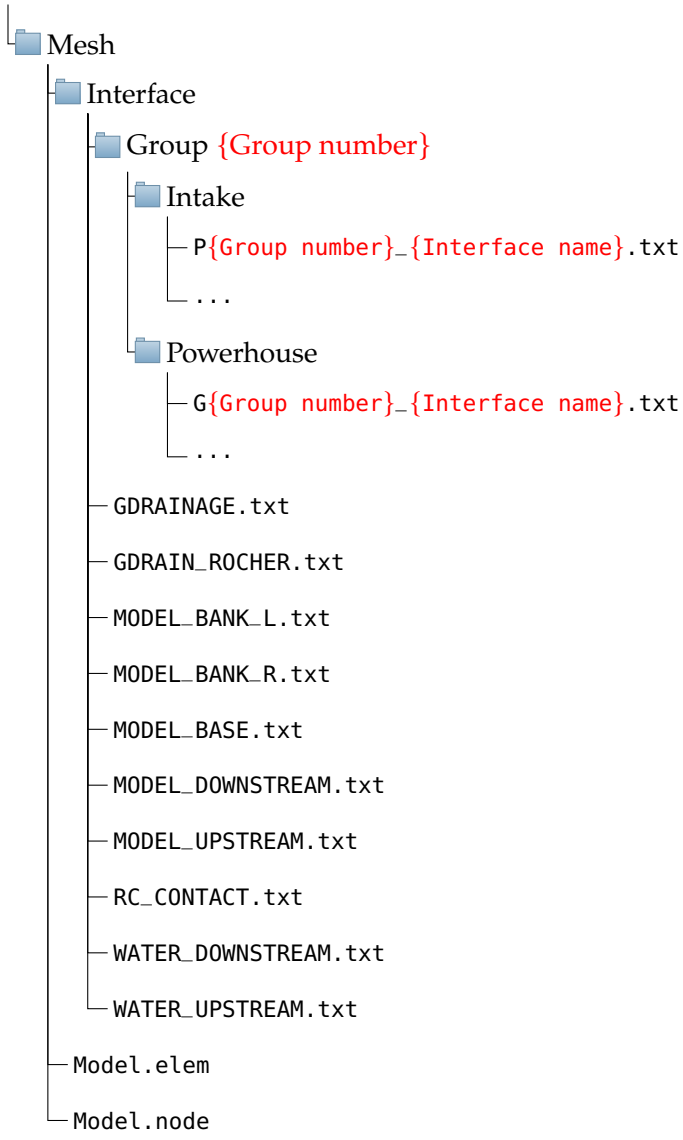

The mesh is separated in two files. The file *Model.node* contains the list of nodes and is defined as follows:

[Model.node]

Node number	X coordinate	Y coordinate	Z coordinate
1	922.9344482000	1244.778198000	11.54189873000
...	...	...	...

The file *Model.elem* contains the list of elements and is defined as follows:

[Model.elem]

i	j	k	l	m	n	o	p	Mesh group number
934	6003	933	933	24431	24431	24431	24431	1
...	...	...	...	...	...	...	...	...

The mesh group number corresponds to the different power-units geometry as defined in table 5.1.

Table 5.1: Mesh group number

Number	Description
1	Foundation
2	Intake #11
3	Power unit #11
4	Intake #12
5	Power unit #12
6	Intake #13
7	Power unit #13

The files in the folder *Interface* with the extension *.txt* are the mesh nodal boundaries given in the form of a list of nodes. The name of the boundaries and their corresponding definition are displayed in figures 5.2 and 5.3.

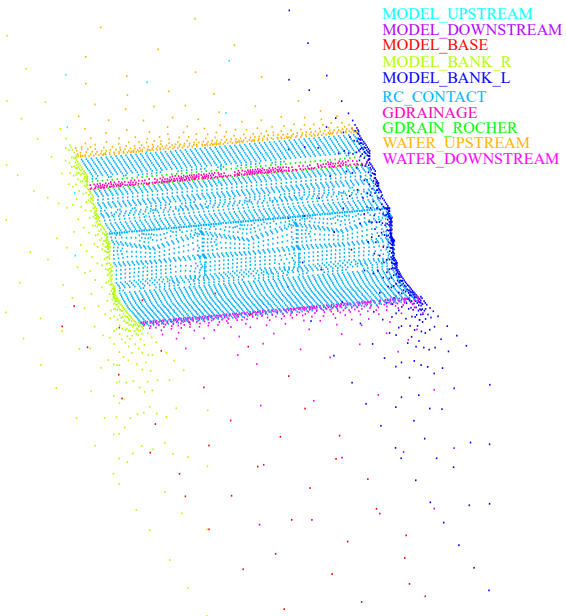

Figure 5.2: Nodal boundaries definitions

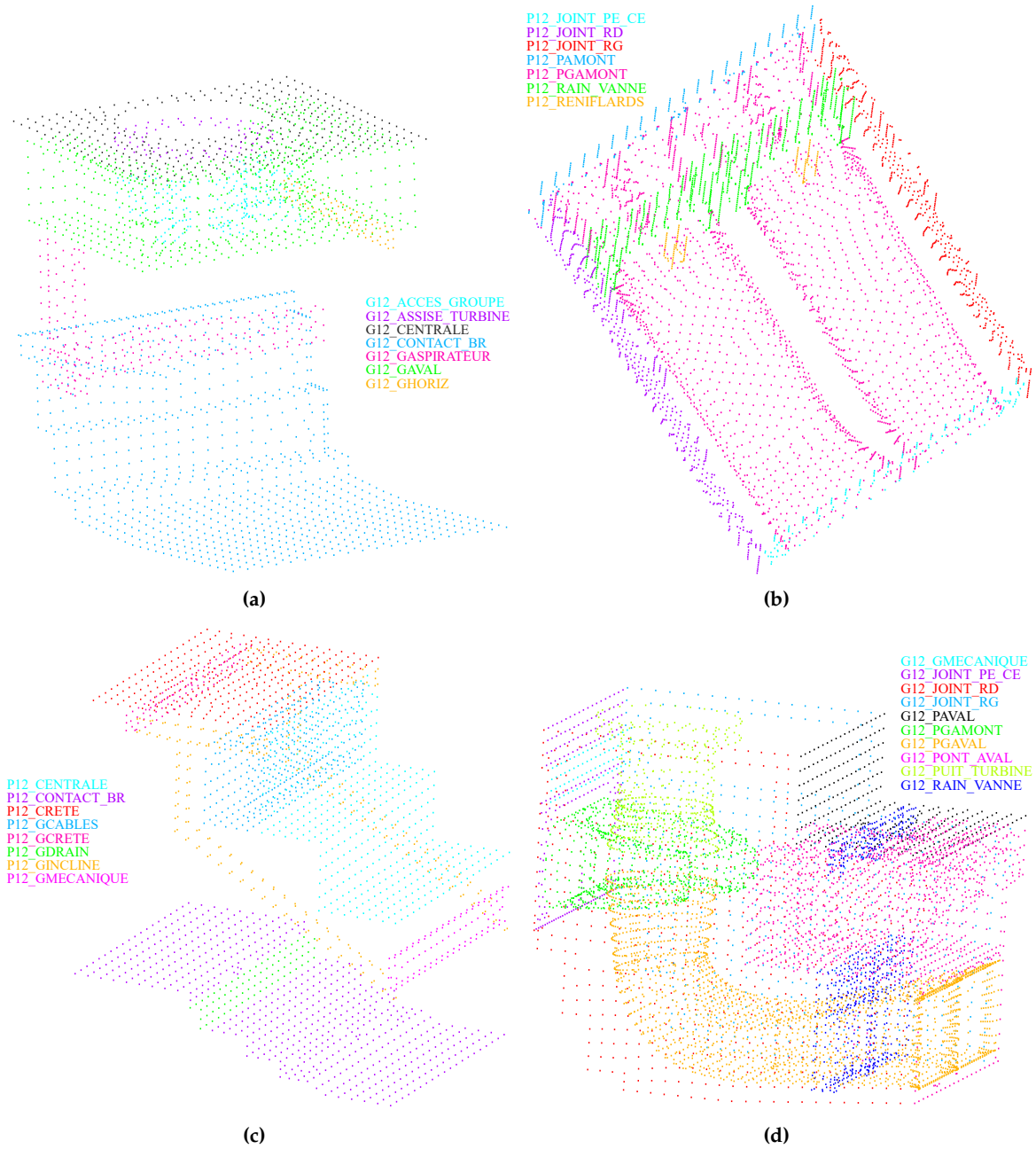

Figure 5.3: Nodal boundaries definitions (cont.)

5.3 Concrete reinforcement

For each power unit, the IGES CAD file containing the reinforcements represented by curves and lines is given with the following hierarchy:

- Reinforcement
  - Group {Group number}
    - Intake
      - CENT1_GR{Group number}_{Diameter}po.{Shape}.{Steel grade}.iges
      - ...
    - Powerhouse
      - PREC1_PE{Group number}_{Diameter}po.{Shape}.{Steel grade}.iges
      - ...

Where:

- {Group number} is the power unit number;
- {Diameter} is the bar diameter in inches;
- {Shape} is the bar shape (r:round, c:square);
- {Steel grade} is the steel grade (refer to section 2.6).

5.4 Temperature boundary conditions data

The temperature data for the four defined zones is given in the file ***Temperature.xlsx***. They are given on a daily average temperature basis. It is assumed that these temperatures can be repeated each year.

- Data
  - Temperature.xlsx

5.5 Topographic data

The available data for the monitoring points identified as 1250D160, 1295Q099, 1250U097 are given in the file ***Topographic Displacements.xlsx***. The topographic auscultation system was implemented in 1973, therefore the first 40 years of data was not recorded. To calibrate the model, it is suggested to shift the data to match the total displacement computed on the first day of acquisition.

- Data
  - Topographic Displacements.xlsx

References

[1] R. Esposito and M. A. N. Hendriks. 'Literature review of modelling approaches for ASR in concrete: a new perspective'. In: *European Journal of Environmental and Civil Engineering* 23.11 (2019), pp. 1311–1331. DOI: 10.1080/19648189.2017.1347068 (cited on page 1).

[2] William L. Oberkampf and Christopher J. Roy. *Verification and Validation in Scientific Computing*. Cambridge University Press, 2010 (cited on page 1).

[3] 'Terminology for model credibility'. In: *SIMULATION* 32.3 (1979), pp. 103–104. DOI: 10.1177/003754977903200304 (cited on page 2).

[4] Department of Defense. *DoD Instruction 5000.61: Modeling and Simulation (MS) Verification*. Department of Defense, 2018 (cited on page 2).

[5] American Institute of Aeronautics and Astronautics. *AIAA Guide for the Verification and Validation of Computational Fluid Dynamics Simulations*. AIAA G.: American Institute of Aeronautics and Astronautics. American Institute of Aeronautics and Astronautics, 1998 (cited on page 2).

[6] American Society of Mechanical Engineers. *Guide for Verification and Validation in Computational Solid Mechanics*. ASME V&V. American Society of Mechanical Engineers, 2006 (cited on page 2).

[7] M.C. Anderson et al. *Concepts of Model Verification and Validation*. Los Alamos National Laboratory, 2004 (cited on page 2).

[8] Xavier Molin and Christine Noret. 'Theme A: Effect of concrete swelling on the equilibrium and displacements of an arch dam'. In: *XI ICOLD Benchmark Workshop On Numerical Analysis Of Dams, Valencia, Spain*. 2011 (cited on page 2).

[9] P. Masarati, G. Mazzà, and M. Meghella. 'Theme A: Evaluation of alkali-aggregate reaction effects on the behaviour of an Italian hollow gravity dam'. In: *VIII ICOLD Benchmark Workshop On Numerical Analysis Of Dams, Wuhan, Hubei, P.R.China*. 2005 (cited on page 2).

[10] ENEL/HYDRO - Polo Idraulico e Strutturale. 'Theme A: Evaluation of AAR effects on the structural behaviour of an arch dam: interpretation of the measured bahaviour and forecasting of the future trend'. In: *VI ICOLD Benchmark Workshop On Numerical Analysis Of Dams, Salzburg, Austria*. 2001 (cited on page 2).

[11] V.E. Saouma. *Diagnosis & Prognosis of AAR Affected Structures: State-of-the-Art Report of the RILEM Technical Committee 259-ISR*. RILEM State-of-the-Art Reports. Springer International Publishing, 2020 (cited on page 2).

[12] J. Bear and Y. Bachmat. *Introduction to modeling of transport phenomena in porous media*. Vol. 4. Jan. 1990 (cited on page 9).

[13] M. Mainguy, O. Coussy, and R. Eymard. *Modélisation des transferts hydriques isothermes en milieu poreux: application au séchage des matériaux à base de ciment*. Études et recherches des Laboratoires des ponts et chaussées. Série Ouvrages d'art. Laboratoire central des ponts et chaussées, 1999 (cited on page 9).

[14] M. Th. van Genuchten. 'A Closed-form Equation for Predicting the Hydraulic Conductivity of Unsaturated Soils'. In: *Soil Science Society of America Journal* 44.5 (1980), pp. 892–898. DOI: 10.2136/sssaj1980.03615995004400050002x (cited on pages 9, 12).

[15] V. Baroghel-Bouny et al. 'Characterization and identification of equilibrium and transfer moisture properties for ordinary and high-performance cementitious materials'. In: *Cement and Concrete Research* 29.8 (1999), pp. 1225–1238. DOI: 10.1016/S0008-8846(99)00102-7 (cited on page 9).

[16] D. Pirtz, Berkeley. Structural Engineering Laboratory University of California, and United States. Army. Corps of Engineers. Walla Walla District. *Creep Characteristics of Mass Concrete for Dworshak Dam*. SESM Report. Structural Engineering Laboratory, University of California, 1968 (cited on page 14).